ANL-HEP-CP--89-107

DE90 002207

Phenomenology of Heavy Quark Production*

EDMOND L. BERGER
High Energy Physics Division
Argonne National Laboratory
Argonne, IL 60439

Abstract

A review is presented of heavy quark production in $\bar{p}p$, $\pi^- p$, and pp interactions at fixed target and collider energies. Calculations of total cross sections and of single quark inclusive differential cross sections $d^2\sigma/dk_T dy$ are described including contributions through next-to-leading order in QCD perturbation theory. Comparisons with available data on charm and bottom quark production show good agreement for reasonable values of the charm and bottom quark masses and other parameters. Predictions and open issues in the interpretation of results are summarized. A brief discussion is presented of signatures, backgrounds, and expected event rates for top quark production.

*Work supported by the U.S. Department of Energy, Division of High Energy Physics, Contract W-31-109-ENG-38. To be published in the Proceedings of the IX Physics in Collision Conference, Jerusalem, June 19–22, 1989.

1. Introduction

The specification of reliable cross sections for heavy quarks, including their production spectra in longitudinal and transverse momentum, and comparisons with data test the quantum chromodynamic (QCD) mechanisms by which all heavy objects are expected to be produced. Strategies in the search for new flavors such as top are predicated on best estimates of cross sections and of momentum distributions in phase space not only of the new flavor but, perhaps more importantly, of lighter flavors which contribute deceptive backgrounds. Those considering hadronic experiments to establish flavor-antiflavor mixing and possible CP violation require a detailed understanding of expected production spectra.

A significant result reported during the past year was the completion[1] of a calculation, through order α_s^3 in QCD perturbation theory, of the inclusive single heavy quark production cross section differential in the transverse momentum k_T and rapidity y of the heavy quark. Here α_s is the running coupling strength in QCD. This result follows the earlier publication[2] of the cross section through order α_s^3 integrated over all k_T and y. Explicit comparisons with data have also been made[3,4]. In this paper I summarize comparisons of the $O(\alpha_s^3)$ cross sections with data on hadroproduction of charm and bottom, and I include several predictions and suggestions for new measurements. The $O(\alpha_s^3)$ contributions are larger in many cases of interest than the $O(\alpha_s^2)$ terms. Not yet available are $O(\alpha_s^3)$ predictions for momentum correlations[5] between the heavy Q and heavy $\bar{Q}$ for values of transverse momentum k_T greater than the quark mass m_Q. These are eagerly awaited inasmuch as the $O(\alpha_s^3)$ $Q\bar{Q}$ jet contributions provide different event topologies[6,7] when $k_T \gg m_Q$. These distributions are important, especially at collider energies, for a proper estimation of the bottom quark background to a possible top quark signal.

In Section 2, I provide a brief summary of the results of the $O(\alpha_s^3)$ computation. Comparisons with data on charm production and on bottom production are presented in Secs. 3 and 4. Comments on top quark production are made in Sec. 5, and conclusions are summarized in Sec. 6.

2. Cross Sections

In hadron hadron interactions, the lowest order parton-parton subprocesses leading to production of a pair of heavy quarks are $q\bar{q} \to Q\bar{Q}$ and $gg \to Q\bar{Q}$. The square of the invariant matrix element for these two-to-two subprocesses is proportional to α_s^2, where $\alpha_s = g^2/4\pi$ and g is the coupling strength in QCD. In QCD, α_s is a logarithmic function of the factorization/renormalization/evolution scale Q, which is only determined to be of order the mass m_Q of the heavy quark. Additional subprocesses enter in the next order in the QCD perturbation expansion. These include $q\bar{q} \to Q\bar{Q}g$, $gg \to Q\bar{Q}g$, $gq \to Q\bar{Q}q$, and $g\bar{q} \to Q\bar{Q}\bar{q}$, and they provide different event topologies.

The total cross section for $ab \to Q\bar{Q}X$, the inclusive production of a pair of heavy quarks, is

$$\sigma_{ab}(s) = \sum_{ij} \int dx_1 \int dx_2 f_i^a(x_1, Q^2) f_j^b(x_2, Q^2) \hat{\sigma}_{ij}(\hat{s}, Q^2). \tag{1}$$

In this equation, $f_i^a(x_1, Q^2)$ represents the density of partons of type i in incident hadron a; $\hat{s} = x_1 x_2 s$ is the square of the energy in the parton-parton collision. The hard scattering cross section $\hat{\sigma}_{ij}$ is written as

$$\hat{\sigma}_{ij}(\hat{s}, Q^2) = \frac{\alpha_s^2(Q^2)}{m_Q^2} F_{ij}\left(\rho, \frac{Q^2}{m_Q^2}\right), \tag{2}$$

where $\rho = 4m_Q^2/\hat{s}$. The dimensionless functions F_{ij} are expressed in the form

$$F_{ij}\left(\rho, \frac{Q^2}{m_Q^2}\right) = F_{ij}^{(0)}(\rho) + 4\pi\alpha_s(Q^2)\left[F_{ij}^{(1)}(\rho) + \bar{F}_{ij}^{(1)}(\rho) \ln \frac{Q^2}{m_Q^2}\right] + O(\alpha_s^2). \tag{3}$$

Explicit expressions for the set of functions $F_{ij}^{(0)}$, $F_{ij}^{(1)}$, and $\bar{F}_{ij}^{(1)}$ may be found in Ref. 2.

Several sources of uncertainty beset attempts to make definite predictions. These include choice of the heavy quark mass; choice of parton densities (particularly the gluon density); and specification of the evolution scale Q^2. The last is an intrinsic theoretical uncertainty. For calculations of total cross sections, there is only one scale in the problem, and it is "natural" to expect Q to lie in the range $m_Q/2 \lesssim Q \lesssim 2m_Q$. Phenomenological results are most unambiguous and reliable in cases in which they do not show sensitivity

to the choice of Q. When the cross section is computed to order α_s^3, changes in Q in the vicinity of m_Q result in "systematic errors" of order α_s^4. These differences are not always small. There appears to be no general evidence for the choice of an optimized evolution scale for heavy flavor production[4]. For calculations of the cross section differential in the transverse momentum k_T of the heavy quark, a convenient choice of scale is $Q^2 = m_Q^2 + k_T^2$.

For many cases of practical interest the QCD contributions in order $O(\alpha_s^3)$ are large. The ratio K of the full cross section computed through order α_s^3 to the result obtained in lowest order, order α_s^2, is defined as

$$K = \sigma\left(O(\alpha_s^2) + O(\alpha_s^3)\right) / \sigma\left(O(\alpha_s^2)\right). \tag{4}$$

I will summarize values of K for specific cases below. Although K is large numerically, it is remarkable that K does not appear to vary significantly[1] over most of the range of k_T and y.

Examples of calculations of top and bottom quark production are shown in Fig. 1 for $\bar{p}p \to QX$ at $\sqrt{s} = 1.8$ TeV. These figures illustrate the important predictions that the average transverse momentum of a heavy quark $\langle k_T \rangle$ grows with m_Q and that $\langle k_T \rangle \simeq m_Q$. Phase space and parton density restrictions reduce the value of $\langle k_T \rangle$ at fixed target energies[3,5–7]. At $\sqrt{s} = 1.8$ TeV, the K factors are about 2.5 for bottom quark production and about 1.5 for top quark production ($m_t = 80$ GeV) in $\bar{p}p$ interactions.

3. Hadroproduction of Charm

In Fig. 2 I present calculations of cross sections for charm quark production in pp interactions at fixed target energies[3]. Values of K are typically 3 for charm production in $\pi^- p$ and pp interactions at fixed target energies. It has been known for some years that the lowest order calculations in QCD provide cross sections which are significantly below experimental measurements. The large increase provided by the $O(\alpha_s^3)$ contributions helps to remedy this discrepancy.

The data in Fig. 2 are from the LEBC-EHS[8] and LEBC-MPS[9] experiments. Beginning with the measured $D/\bar{D}$ inclusive and $D\bar{D}$ pair cross sections, Goshaw[10] obtained estimates of the cross sections for $pp \to c\bar{c}X$. His value is $\sigma(pp \to c\bar{c}X) = 14$ to 23 μb at

$p_{\rm lab}$ = 400 GeV/c. Using his algorithm and the value $\sigma(D/\bar{D}) = 44^{+10}_{-8}$ μb at 800 GeV/c reported by G. Mendez[9], I find $\sigma(pp \to c\bar{c}X)$ = 22 to 37 μb at $p_{\rm lab}$ = 800 GeV/c. Cross sections have been determined in many other experiments. However, I choose not to show them in Fig. 2 because many of those measurements were made with nuclear targets, and the precise nuclear A dependence is not known in each case.

A glance at Fig. 2 shows the considerable sensitivity of predictions to the choices of the charm quark mass m_c and of the parton densities. For a given set of parton densities, a decrease of the mass from m_c = 1.5 GeV to m_c = 1.2 GeV results in an increase in cross section by about a factor of three. For a given m_c, there is about a factor of two increase in predicted cross section when the Duke-Owens[11] set 1 (DO 1) parton densities are used instead of the Martin-Roberts-Stirling[12] set 1 (MRS 1). Since the $c\bar{c}$ cross section is proportional to α_s^2, a substantial fraction of the difference of predicted yields is attributed to the different values of Λ in the DO 1 and MRS 1 parametrizations[3].

At the ISR energy of $\sqrt{s}$ = 63 GeV, we may use the DO 1 (m_c = 1.5 GeV) and MRS 1 (m_c = 1.2 GeV) curves in Fig. 2 to bracket uncertainties from below and above. I estimate that $\sigma(pp \to c\bar{c}X;\ \sqrt{s} = 63$ GeV) lies most likely in the range of 55 to 100 μb. Even with $O(\alpha_s^3)$ contributions included, it is difficult to accommodate a charm cross section greater than $\sim$130 μb at $\sqrt{s} = 63$ GeV.

Calculations for $\pi^- p \to c\bar{c}X$ are presented in Ref. 3, and those for photoproduction are available in Ref. 13. The results in Fig. 2 and those for $\pi^- p \to c\bar{c}X$ and $\gamma N \to c\bar{c}X$ demonstrate that defensible QCD calculations reproduce the energy dependence and the magnitude of the measured total charm cross section at fixed target energies. However, because of the sensitivity to the choice of the parton densities, we cannot use the results to "pin down" the charm quark mass appropriate in perturbative calculations to better than $1.2 < m_c < 1.5$ GeV. It does appear possible, however, to discard a mass as large as m_c = 1.8 GeV. The agreement between theory and data in Fig. 2 is an indication that charm production may be on the way towards being "understood" in terms of perturbative QCD. There are important open issues[3], however, including: discomfort with the large size of the K factor; possible leading particle effects in the experimental longitudinal momentum distribution of charm *particles*, $d\sigma/dx_F$, not reproduced by perturbative calculations of charm *quark* production; the nuclear dependence of charm production; and higher-twist

effects known to be important in deep-inelastic lepton scattering for values of $Q^2 \simeq 4m_c^2$.

I would emphasize the special importance of experiments to determine the nuclear A dependence of charm production. The incoherence/factorization assumptions inherent in applications of perturbative QCD lead to the expectation of an approximately linear dependence on A. If measurements were to establish that $\sigma_{c\bar{c}} \propto \sigma_0 A^\alpha$ with α substantially less than 1, e.g. $\alpha \lesssim 0.9$, then the applicability of perturbative QCD would be seriously in doubt. An interpretation of values of $\alpha < 1$ is proposed in Ref. 14. As data samples become larger, it should be possible to study charm production at large k_T and to examine $c\bar{c}$ momentum correlations[5].

4. Hadroproduction of Bottom

In Figs. 3 and 4 calculations of $b\bar{b}$ pair cross sections are shown as a function of energy in $\pi^- p$ and $\bar{p}p$ interactions. Predictions for $pp \to b\bar{b}X$ may be found in Refs. 1, 3, and 4. As in the case of charm discussed in Sec. 3, the contributions in order α_s^3 are significant. At fixed target energies the value of K in pp interactions is larger than in $\pi^- p$ interactions, related to the more important role of gluon initiated subprocesses in pp interactions[3].

In Fig. 3, I present the total $b\bar{b}$ pair cross section in $\pi^- p$ interactions at fixed target energies for a particular choice of bottom quark mass $m_b = 5$ GeV. The one datum is a measurement of the CERN WA78 collaboration[15]. Originally the WA78 group had published[19] a value of $\sigma(\pi^- N \to b\bar{b}X;\ p_{\rm lab} = 320\ {\rm GeV}) = 4.5 \pm 1.4 \pm 1.4$ nb per nucleon. Subsequent reevaluations were made of their overall normalization reference as well as of their acceptance and efficiency based on a model which incorporates production properties in transverse and longitudinal momenta consistent with those predicted[5,6] in perturbative QCD. These improvements result in a reduction of the cross section[15] to 3.2 ± 1.1 nb per nucleon if the $b\bar{b}$ mixing parameter χ is fixed at $\chi = 0.2$. A linear dependence of σ on nuclear baryon number A was assumed, as is reasonable for bottom quark production. Another group[20] reported observation of a signal consistent with bottom production and quotes a "model dependent $b\bar{b}$ production cross section" $\sigma(\pi^- N \to b\bar{b}X;\ p_{\rm lab} = 286\ {\rm GeV}) = 14^{+7}_{-6}$ nb per nucleon, considerably larger than that of the CERN WA78 collaboration. An analysis by the WA78 collaboration[15] shows that the difference between the cross sections quoted by

WA78 and NA10 is most likely due to different model assumptions, not to differences in the data. The model adopted by the NA10 group to simulate $B\bar{B}$ production is questionable[3]; it incorporates correlations considerably at variance with QCD expectations[5].

The calculations shown in Fig. 3 are appropriate for $\pi^- p \to b\bar{b}X$ whereas the one datum is derived from interactions on a uranium target. The theoretical results should be modified for the fact that the target is a mixture of neutrons and protons. This effect was studied in Ref. 7 where I showed that the cross section per average nucleon is *smaller* than the cross section for production from proton targets; the factors are 0.68, 0.80, and 0.87 at $p_{\rm lab} = 200$, 400, and 600 GeV/c.

For $\pi^- p \to b\bar{b}X$ in the momentum range 300 to 600 GeV/c, there is about a factor of two decrease in the total cross section when the evolution scale is increased from $Q^2 = m_b^2$ to $Q^2 = 4m_b^2$. Comparison with the datum in Fig. 3 favors the choice $Q^2 = 4m_b^2$ if $m_b = 5$ GeV. As discussed in Refs. 6 and 7, over the range $400 < p_{\rm lab} < 1000$ GeV/c, the expected cross section $\sigma(pp \to b\bar{b}X)$ is decreased by about a factor of two when the b quark mass is increased from $m_b = 5$ GeV to 5.4 GeV and increased by about a factor of two if the b quark mass is decreased from 5 GeV to 4.6 GeV.

Predictions of the total cross section at collider energies are shown in Fig. 4. Taken at face value, the curves indicate a fairly large spread in predictions associated with the choice of different parameters. For bottom production at $\sqrt{s} \gtrsim 200$ GeV, the pp and $\bar{p}p$ cross sections are nearly equal. The only measurement of bottom production at $\bar{p}p$ collider energies is that reported by the UA1 collaboration based on an analysis of muon production. The $b\bar{b}$ pair cross section extrapolated to all phase space[18] is $\sigma(p\bar{p} \to b\bar{b}X) = 10.2 \pm 3.3\mu$b in fine agreement with expectations and tending to favor $m_b \gtrsim 4.75$ GeV and $\mu \equiv Q \gtrsim m_b$.

The integral transverse momentum spectrum $\sigma(k_T \geq k^{\rm min})$ is shown in Fig. 5 for $\bar{p}p \to bX$ at $\sqrt{s} = 630$ GeV. Theoretical predictions are presented as a band of values corresponding to ranges of uncertainty in m_b, the evolution scale, the parton densities, and Λ. The data are from the UA1 experiment[18]. Good agreement between theory and experiment is apparent for $k^{\rm min} \lesssim 15$ GeV. There may be a discrepancy at larger values of $k^{\rm min}$. However, several remarks are in order. The data in Fig. 5 appear *not* to have been corrected for smearing effects in k_T associated with experimental resolution functions. Smearing tends to broaden steeply falling k_T spectra. Second, in the data, in addition to hadronic production

mechanisms, there are other sources of b's with large k_T such as $Z^0 \to b\bar{b}$ not included in the theoretical calculation. Third, single and double muon momentum spectra are measured, and a multi-step procedure is used to work back from these data to the b quark momentum distribution shown in Fig. 5. The three data points with $k^{\rm min} \geq 15$ GeV are based entirely on the measured inclusive single muon spectrum. It is not clear that experimental systematic uncertainties are properly estimated. Finally, on the theoretical side, whenever two different large momentum scales are present (here, k_T and m_Q), contributions arise proportional to $[\alpha_s \ln(k_T/m_Q)]^n$. Such terms must be summed if $\alpha_s \ln(k_T/m_Q)$ becomes of order unity[1]. These contributions will either soften or harden the $k^{\rm min}$ distribution. More detailed analyses of larger data sets at both $\sqrt{s} = 630$ GeV and $\sqrt{s} = 1.8$ TeV as well as theoretical studies of the $\alpha_s \ln(k_T/m_Q)$ series should resolve these questions.

At $\sqrt{s} = 1.8$ TeV, the integral k_T cross section $\sigma(\bar{p}p \to bX)$ is expected to exceed 5 μb for $k_T \geq 5$ GeV and $|y| < 1$. The CDF collaboration currently has an integrated luminosity of ~ 4.7 pb^{-1} on tape at $\sqrt{s} = 1.8$ TeV. Correspondingly, more than 2×10^7 $b\bar{b}$ pairs should have been produced in the range $|y| \leq 1$ and $k_T \geq 5$ GeV and should be available for analysis in those tapes. The b events are of interest in their own right (QCD dynamics, correlations, mixing,...) and must be understood as a background in searches for new physics including, but not limited to top.

In lowest order perturbation theory simple momentum correlations are expected between the heavy Q and $\bar{Q}$ produced in $hN \to Q\bar{Q}X$. For example, the transverse momentum vectors should be equal in magnitude but oppositely directed: $\vec{p}_{TQ} = -\vec{p}_{T\bar{Q}}$. Thus, the pair transverse momentum is expected to be small ($|\vec{p}_{TQ} + \vec{p}_{T\bar{Q}}| \lesssim O(1\ \text{GeV})$), and the distribution in the difference $\Delta\phi$ between the azimuthal angles of the Q and $\bar{Q}$ in the transverse plane should display a peak near $\Delta\phi = 180°$. Next to leading order contributions in QCD change these expectations. "Gluon splitting" terms produce events in which $\Delta\phi \simeq 0$, and "flavor excitation" terms provide a broad distribution in $\Delta\phi$. The distribution in the pair transverse momentum $|\vec{p}_{TQ} + \vec{p}_{T\bar{Q}}|$ is broadened. A full $O(\alpha_s^3)$ calculation of these correlations has not been published, but Monte Carlo programs can be used to estimate the role of the next to leading order terms.

An analysis was presented in Ref. 5 of the expected correlations in longitudinal momentum between a heavy quark Q and its antiquark $\bar{Q}$ produced in hadronic interactions at

fixed target and collider energies. For a sufficiently heavy quark (e.g. bottom), the nature of these correlations should be predicted reliably by lowest-order perturbative QCD as long as the transverse momentum k_T is not large in comparison with m_Q. The QCD Born cross sections have simple dependences on the difference Δy of the rapidities of the Q and $\bar{Q}$. They show that the basic QCD dynamics favors *positive*, albeit *broad* correlations in rapidity. When sufficient phase space is available, as it is at collider energies, the two particle rapidity distribution $d^2\sigma/dy_1dy_2$, considered as a function of y_2 for fixed y_1, should therefore display at peak at y_2 near y_1. However, $d^2\sigma/dy_1dy_2$ is expected to be a broad distribution. Depending upon the rapidity y_1 of an identified Q, the "correlation length" between the produced Q and its accompanying $\bar{Q}$ may exceed by a factor of two the ~ 2 units which is typically assumed. This statement has implications for the design of future detectors and for the evaluation of acceptances in analyses of current data.

Doubly differential distributions in rapidity and in Feynman x_F are presented in Ref. 5 for bottom quark production at typical fixed target and collider energies. One conclusion evident from a comparison of results at $\sqrt{s} = 630$ GeV and $\sqrt{s} = 1.8$ TeV is that the average value of the rapidity difference is expected to increase. Considered as a function of y_2 at $y_1 = 0$, the predicted full widths at half maximum of $d^2\sigma/dy_1dy_2$ are 3.6 and 4.2, respectively. At fixed target energies, the relatively limited phase space mitigates against observation of strong correlations. In terms of the Feynman x_F variable, one expects a slight residual anticorrelation[5]. Comparison of these predictions with forthcoming data should provide valuable additional insight into the applicability of perturbative QCD for heavy quark production.

5. Top Quark

For a fixed value of $\sqrt{s}$, the contributions through $O(\alpha_s^3)$ in perturbative QCD result in smaller increases in predicted yields as the quark mass is increased. For example, at $\sqrt{s} = 630$ GeV, *typical* K factors[2] are in the range $1.2 \lesssim K \lesssim 1.7$ for a top quark of mass $m_t = 40$ GeV and $1.1 \lesssim K \lesssim 1.3$ for $m_t = 80$ GeV. At $\sqrt{s} = 1.8$ TeV, the numbers are $1.3 \lesssim K \lesssim 1.8$ at $m_t = 40$ GeV and $1.2 \lesssim K \lesssim 1.7$ at $m_t = 80$ GeV.

In addition to the hadronic mechanisms discussed in this review, production through decay of intermediate vector bosons must also be considered; e.g. $\bar{p}p \rightarrow W^{\pm}X$, $W \rightarrow t\bar{b}$

and $\bar{p}p \to Z^0 X$, $Z^0 \to t\bar{t}$. Cross sections are presented in Fig. 6 as a function of the mass of the top quark[6,7]. At the CERN collider energy of $\sqrt{s} = 630$ GeV, the intermediate W mechanism is dominant for $40 < m_t < 78$ GeV. At Fermilab Tevatron collider energies, hadronic production is dominant for all values of m_t. For an integrated luminosity of 1 pb^{-1} at $\sqrt{s} = 1.8$ TeV, the cross sections in Fig. 6 correspond to the production of 10^4 $t\bar{t}$ pairs if $m_t = 40$ GeV and 100 $t\bar{t}$ pairs if $m_t = 100$ GeV.

A favorite signature for top production is the identification of an isolated lepton plus at least two hadronic jets. The overall branching fraction for the decay $t \to b\ell\nu$; $\bar{t} \to$ hadronic jets is $2 \times 2 \times (1/9) \times (2/3) \simeq 0.3$ ($\ell = e$ or μ).

The severity of backgrounds is best appreciated by an examination of the integral transverse momentum spectrum $\sigma_b \left(p_{T,b} > p_{T,b}^{\min}\right)$ for bottom quark production. Motivated by the notion that a bottom quark moving with large $p_{T,b}$ will yield a decay lepton whose transverse momentum is comparable to that arising from the decay of a slowly moving but more massive quark, we may compare $\sigma_b(p_{T,b} > m_t)$ with $\sigma_t(p_{T,t} > 0)$. As shown in Refs. 6 and 7, $\sigma_b(p_{T,b} > 40 \text{ GeV}) > \sigma_t(p_{T,t} > 0, m_t = 40 \text{ GeV})$. Thus, the distribution in transverse momentum of leptons at large $p_{T,\ell}$ is likely to be dominated by backgrounds from the semi-leptonic decay of b and c quarks. Further selections are needed to achieve a signal to background ratio approaching unity. Particularly promising appears to be the distribution in an isolation variable, I, where I is a measure of the total energy within a cone of solid angle about the direction of the identified lepton[21]. For light quarks moving with large transverse momentum, it is likely that hadronic energy associated with the secondary quark (e.g. c in $b \to \ell\nu c$) will be folded forward into the cone of solid angle about the direction of ℓ. Correspondingly, I will be large. By contrast, for decay of a massive t quark, $t \to \ell\nu b$, there is a greater chance of that the lepton ℓ will be isolated in phase space, resulting in a peak near $I = 0$. Precise predictions of the distributions in I associated with both the signal and backgrounds require a refined understanding of the dynamics of the semi-leptonic decay process $Q \to \ell\nu q$.

In their case study of the production of a possible top quark with mass $m_t = 40$ GeV, the UA1 collaboration[21], determined that a selection $I < 2$, in conjunction with other important selections, was necessary to achieve a signal to background ratio of 2 or greater. After all selections are imposed, the UA1 efficiency for detecting a top quark in the muon

channel is 4.6% for a top quark mass of 40 GeV. By implication, about 50 events will be retained of the 10^4 $t\bar{t}$ events in a 1 pb^{-1} sample at $\sqrt{s} = 1.8$ TeV. The efficiency improves as m_t is increased. With larger data samples, it should be possible to move away from reliance on Monte Carlo calculations of the shape and magnitude of the background in the isolation distribution. After leptons are selected in a narrow band of values of the lepton transverse momentum $p_{T,\ell}$, experimental distributions may be made vs. isolation I. Most desirable would be the emergence in the data themselves, for large $p_{T,\ell}$, of a clear peak at small I in distribution of the isolation variable.

If $m_t > m_W$, the dominant background appears to arise from the QCD production of W's in association with hadronic jets[22]. Unconventional decays of the top would make detection even more difficult. These include[23] $t \to bH^+$, $H \to \tau\nu$ or $c\bar{s}$ and[24] $t \to \tilde{t}\tilde{\gamma}$, $\tilde{t} \to b\tilde{W}$. Here H^+ denotes a possible charged Higgs particle, and $\tilde{t}$ denotes the supersymmetry partner of the top quark.

6. Conclusions and Discussion

Heavy flavor production has been advanced to a new level of precision in perturbative QCD now that full next-to-leading order calculations have been completed for the total cross section and for the single quark inclusive cross section. The contributions in order α_s^3 are large in many cases of practical interest. These calculations offer the potential of better agreement with data, but they also raise questions about convergence of the expansion of the cross section in perturbative QCD.

The size of the $O(\alpha_s^3)$ contributions is particularly significant when the integration over phase space is dominated by values of the parton-parton subenergy *either* close to threshold, $\hat{s} \sim 4m_Q^2$, *or* very large, $\hat{s} \gg 4m_Q^2$. Correspondingly, predictions will be most stable in restricted intervals of $2m_Q/\sqrt{s}$. According to these criteria, predictions for top quark production at the current collider energies of $\sqrt{s} = 630$ GeV and $\sqrt{s} = 1.8$ TeV would seem particularly reliable, as would those for bottom quark production at Fermilab fixed target energies. While the large contributions from the $O(\alpha_s^3)$ 2 to 3 subprocesses for $\sqrt{s} \gg 2m_Q$ may appear alarming, they do not *per se* cast doubts on the applicability of perturbation theory for heavy quark production. The higher order 2 to 3 subprocesses are mediated by gluon exchange in the crossed ($\hat{t}$) channel, implying that $\hat{\sigma}_{2\to3}$ approaches a

constant as $\hat{s}$ increases, whereas the lowest order 2 to 2 subprocesses are controlled by heavy quark exchange in the crossed channel, with $\hat{\sigma}_{2\to 2} \to 1/\hat{s}$. Thus, the large contributions at order α_s^3 arise from new subprocesses, with different $\hat{t}$ channel exchanges, not from simple "corrections" to the lowest order subprocesses.

Applicability of the perturbative results requires that the mass of the heavy flavor be "large". Whether charm, with $1.2 < m_c < 1.5$ GeV, satisfies this restriction is not clear. Issues in charm production also include a quantitative understanding of the nuclear A dependence, possible leading particle effects, and quantitative estimates of the role of (additive) higher twist terms, proportional to 1 GeV$/m_Q$. If the reservations discussed above are set aside, the calculations through order α_s^3 may be compared with data on charm production at fixed target energies, as was done in Sec. 3. Good agreement is obtained for values of m_c in the range $1.2 < m_c < 1.5$ GeV. Uncertainties include the choice of $\Lambda_{\rm QCD}$, the magnitude and shape of the gluon density $g(x, Q^2)$ in the relevant interval of x, and the choice of the evolution scale Q^2 in both α_s and the parton densities. Measurements of correlations in rapidity between produced Q and $\bar{Q}$ will provide valuable additional checks on production dynamics[5]. They may be particularly valuable in the case of charm production for separating perturbative effects from those associated with final state interactions.

For bottom production, the scale is set by the relatively large mass of the bottom quark $m_b \simeq 5$ GeV. Perturbative calculations ought to be reliable, and the nuclear dependence should be linear, $\sigma \propto A^1$. Theory and experiment agree at better than the factor of two level at fixed target and collider energies, but only much more precise data over a broad range of energies will permit tighter bounds on the "parameter set" (m_b, Q^2, Λ, and $g(x, Q^2)$). Cross sections from the CDF experiment at $\sqrt{s} = 1.8$ TeV are eagerly awaited. Approved fixed-target experiments on bottom quark production include CERN WA84 πN at 350 GeV and Fermilab E791 πN at 500 GeV, E653 πN at 600 GeV, E771 pN at 800 GeV, and E789 pN at 800 GeV.

Further theoretical study is necessary to better understand the large size of the next-to-leading order contributions. It is desirable to extend present calculations of the $O(\alpha_s^3)$ contributions to a full treatment of the joint Q and $\bar{Q}$ distribution in $hN \to Q\bar{Q}X$ so that $Q/\bar{Q}$ momentum correlations will be fully specified through $O(\alpha_s^3)$. It would also be valuable to incorporate the $O(\alpha_s^3)$ cross sections into a full Monte Carlo simulation program to permit

a detailed investigation of double-tagged events, associated jets, and other properties of events containing heavy quarks.

Acknowledgments

Research done at Argonne National Laboratory is supported by the Department of Energy, Division of High Energy Physics, Contract W-31-109-ENG-38.

References

1. P. Nason, S. Dawson, and R. K. Ellis, Fermilab report FNAL-PUB-89/91-T (April, 1989).

2. P. Nason, S. Dawson, and R. K. Ellis, Nucl. Phys. **B303**, 607 (1988); see also W. Beenakker, H. Kuijf, W. L. Van Neerven, and J. Smith, Phys. Rev. **D40**, 54 (1989).

3. E. L. Berger, "Heavy Flavor Production", Argonne report ANL-HEP-CP-88-26, to be published in the Proceedings of the Advanced Research Workshop on QCD Hard Hadronic Processes, St. Croix, October, 1987.

4. G. Altarelli, M. Diemoz, G. Martinelli and P. Nason, Nucl. Phys. **B308**, 724 (1988).

5. E. L. Berger, Phys. Rev. **D37**, 1810 (1988).

6. E. L. Berger, N[illegible] B (Proc. Suppl.)**1B**, 425 (1988).

7. E. L. Berger, in *Hadrons, Quarks, and Gluons*, Proceedings of the XXII Rencontre de Moriond, Les Arcs, France, edited by J. Tran Thanh Van (Editions Frontières, France, 1987) pp. 3–40.

8. M. Aguilar-Benitez *et al.*, Phys. Lett. **135B**, 237 (1984), **189B**, 476 (1987), and Z. Phys. **C40**, 321 (1988).

9. R. Ammar *et al.*, Phys. Lett. **183B**, 110 (1987); G. Mendez, Duke University, Ph.D. thesis (May, 1989).

10. A. T. Goshaw, "Charm Production from 400 and 800 GeV/c Proton-Proton Collisions", St. Croix, *loc. cit.*

11. D. W. Duke and J. F. Owens, Phys. Rev. **D30**, 49 (1984).

12. A. D. Martin, R. G. Roberts, and W. J. Stirling, Phys. Rev. **D37**, 1161 (1988).

13. R. K. Ellis and P. Nason, Nucl. Phys. **B312**, 551 (1989).

14. S. J. Brodsky and P. Hoyer, SLAC report SLAC-PUB-4978 (May, 1989).

15. G. Penso, WA78 Collaboration, private communication, June, 1989.

16. R. K. Ellis, private communication.

17. M. Diemoz *et al.*, Z. Phys. **C39**, 21 (1988).

18. UA1 Collaboration, C. Albajar *et al.*, Phys. Lett. **213B**, 405 (1988).

19. M. G. Catanesi *et al.*, Phys. Lett. **187B**, 431 (1987).

20. P. Bordalo *et al.*, NA10 Collaboration, Z. Phys. **C39**, 7 (1988).

21. UA1 Collaboration, C. Albajar *et al.*, Z. Phys. **C37**, 505 (1988).

22. H. Baer, V. Barger, H. Goldberg, and R. J. N. Phillips, Phys. Rev. **D37**, 3152 (1988); R. Kleiss, A. D. Martin, and W. J. Stirling, Z. Phys. **C39**, 393 (1988); S. Gupta and D. P. Roy, Z. Phys. **C39**, 417 (1988).

23. V. Barger and R. J. N. Phillips, Phys. Lett. **B201**, 553 (1988).

24. I. Bigi and S. Rudaz, Phys. Lett. **153B**, 335 (1985); H. Baer and X. Tata, Phys. Lett. **167B**, 241 (1986).

FIGURE CAPTIONS

Fig. 1 The predicted differential cross sections $d^2\sigma/dy\,dk_T^2$ as a function of k_T for selected values of rapidity y for (a) bottom quark production, and (b) top quark production, $m_t = 80$ GeV, in antiproton-proton collisions at $\sqrt{s} = 1.8$ TeV, from Ref. 1. The solid lines are the full calculations through order α_s^3, and the dashed lines are lowest order α_s^2 results multiplied by constant K factors of (a) 2.5 and (b) 1.5.

Fig. 2 Cross sections for $pp \to c\bar{c}X$ as a function of the laboratory momentum for two choices of the charm quark mass m_c and two different sets of parton densities. I obtained these results from the full QCD expression through order α_s^3; the evolution scale Q^2 was chosen as $Q^2 = 4m_c^2$. The data at $p_{\rm lab} = 400$ and 800 GeV are derived from measurements by the LEBC-EHS (Ref. 8) and LEBC-MPS (Ref. 9) collaborations.

Fig. 3 Cross section through order α_s^3 for bottom quark production in $\pi^- p$ interactions as a function of laboratory momentum, from Ref. 3. Here $m_b = 5$ GeV, and two choices are made for the evolution scale, $Q^2 = m_b^2$ and $Q^2 = 4m_b^2$. The one datum is the result reported by the WA78 collaboration, Ref. 15.

Fig. 4 Calculations of bottom quark production in proton-antiproton collisions as a function of $\sqrt{s}$, Ref. 16. The full answer through order α_s^3 is shown for three different choices of the QCD scale Λ (5 flavors), the bottom quark mass m, and the factorization scale μ $(= Q)$. The Diemoz *et al.* parton densities were used, Ref. 17. The one datum is from the CERN UA1 collaboration, Ref. 18.

Fig. 5 Integral transverse momentum spectrum $\sigma(k_T > k^{\rm min})$ as a function of the minimum transverse momentum $k^{\rm min}$ of the bottom quark for $\bar{p}p \to bX$ at $\sqrt{s} = 0.630$ TeV, with the rapidity of the bottom quark restricted to the interval $|y| < 1.5$. The data are from the CERN UA1 collaboration, Ref. 18. The solid line is an order α_s^3 calculation from Ref. 1 in which the bottom quark mass is fixed at $m_b = 4.75$ GeV, the evolution scale is $Q^2 = m_b^2 + k_T^2$, and the DFLM set 2 parton densities (Ref. 17) are used with Λ (four flavors)=260 MeV. The dashed lines represent the band of theoretical uncertainty obtained as a result of varying the bottom quark mass, the evolution scale, and the parton densities over the ranges shown on the figure.

Fig. 6 Expected cross sections as a function of the mass of the top quark at $\sqrt{s} = 630$ GeV and $\sqrt{s} = 2$ TeV, order α_s^2 only, from Refs. 6 and 7.

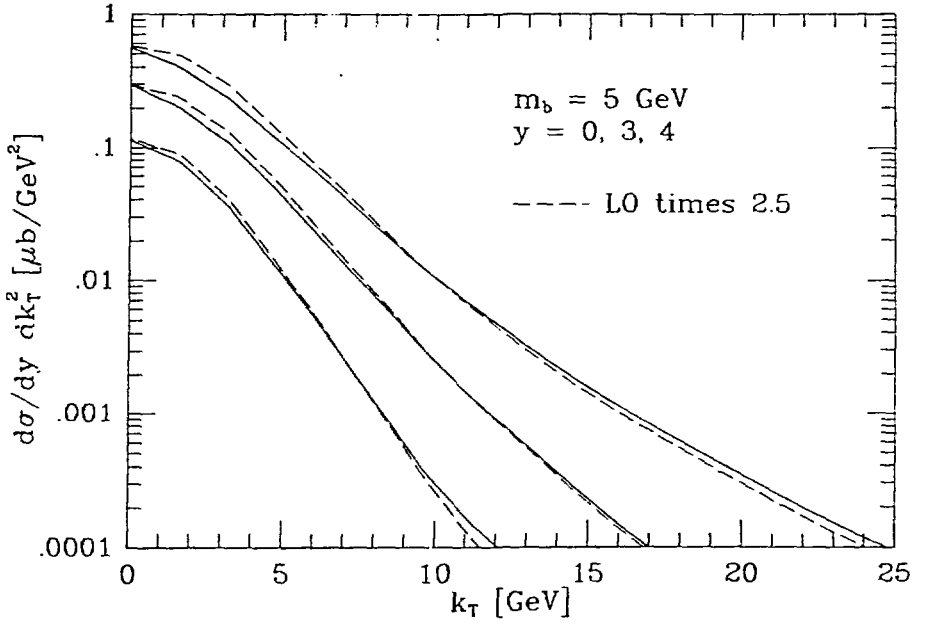
1
.1
.01
.001
.0001
0
5
10
15
20
25
k_T [GeV]
$d\sigma/dy\ dk_T^2$ [μb/GeV^2]
m_b = 5 GeV
y = 0, 3, 4
---- LO times 2.5

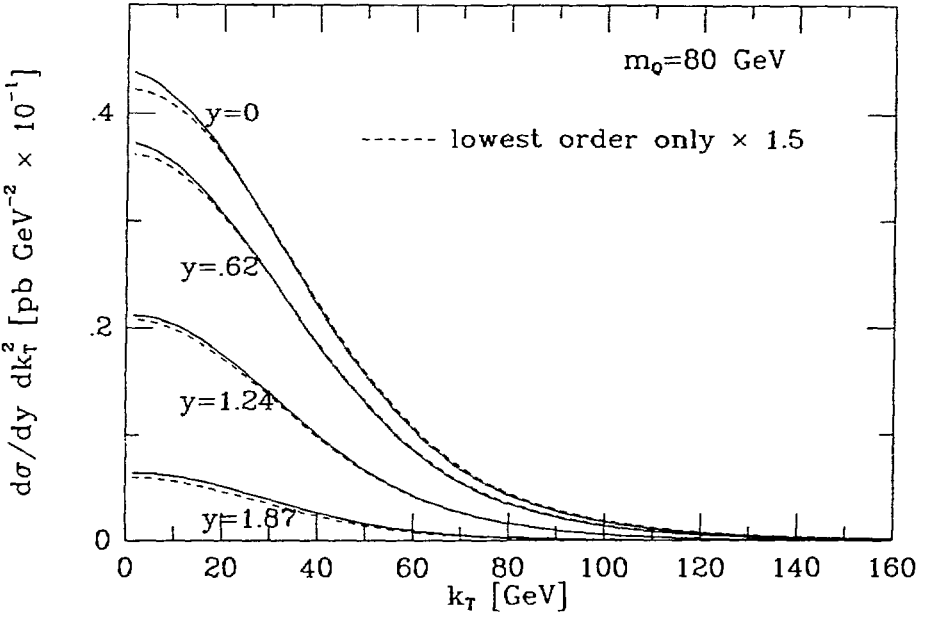
.4
.2
0
0
20
40
60
80
100
120
140
160
k_T [GeV]
$d\sigma/dy\ dk_T^2$ [pb GeV^{-2} × 10^{-1}]
m_Q=80 GeV
y=0
------ lowest order only × 1.5
y=.62
y=1.24
y=1.87

Fig. 1

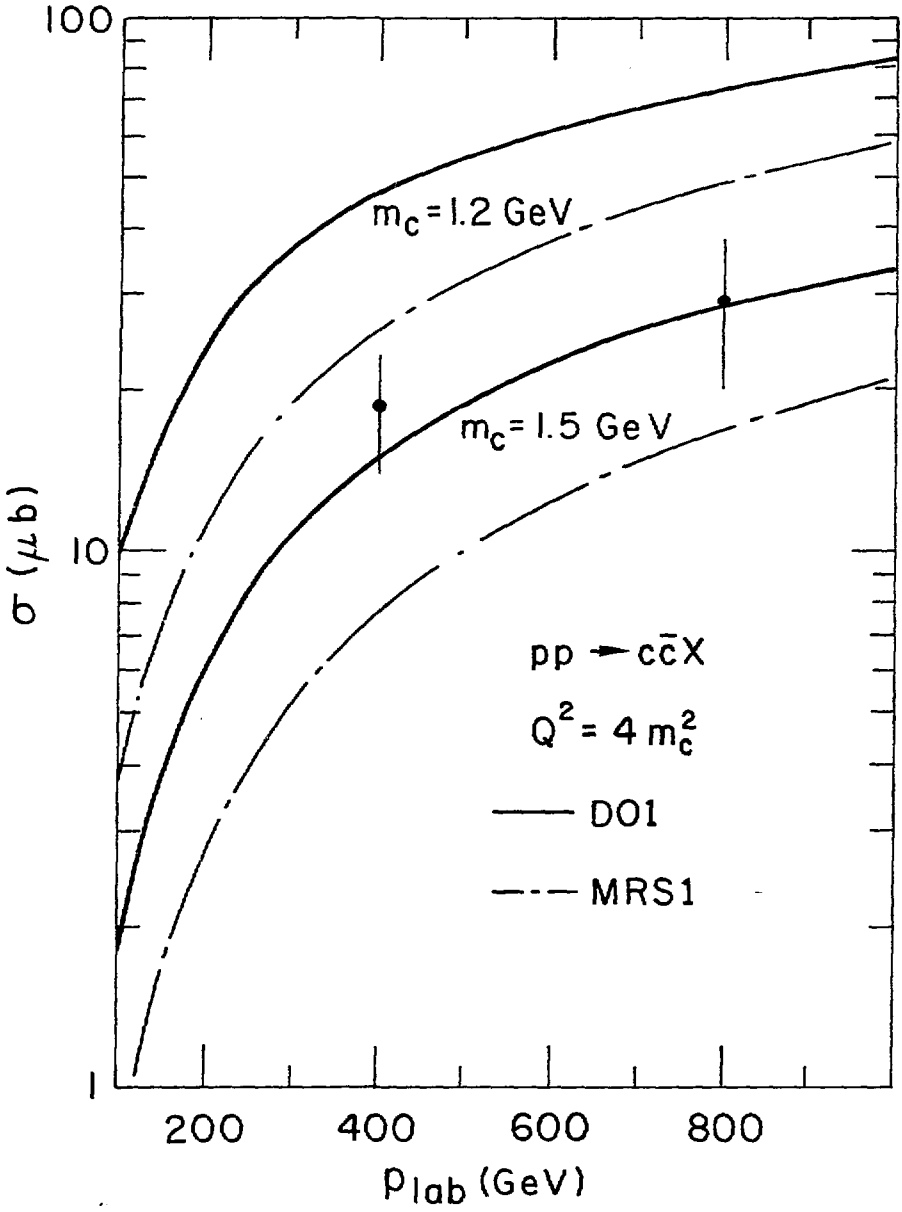
100
10
1
σ (μb)
m_c = 1.2 GeV
m_c = 1.5 GeV
pp → cc̄X
$Q^2 = 4\,m_c^2$
DO1
MRS1
200
400
600
800
p_{lab} (GeV)

Fig. 2

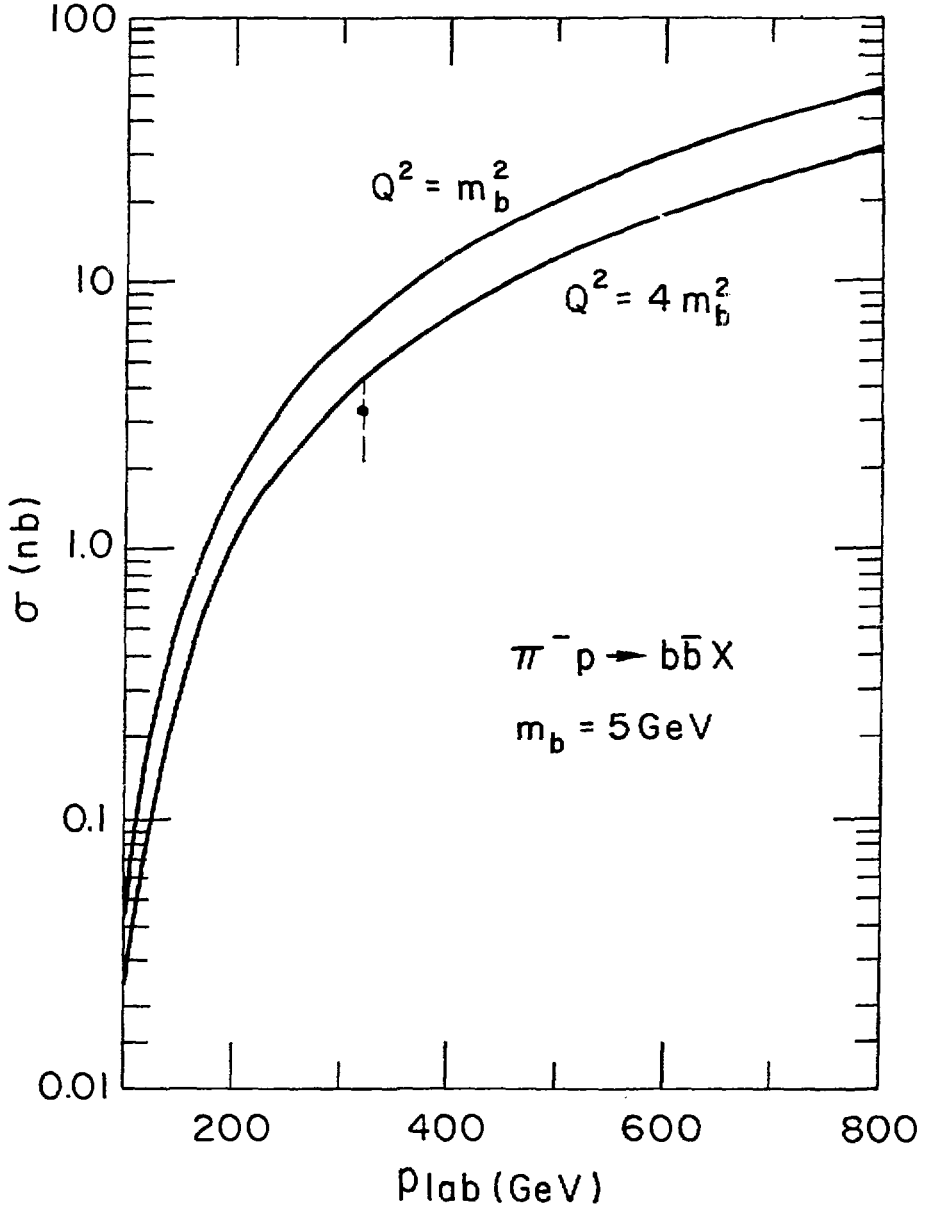
100
10
1.0
0.1
0.01
σ (nb)
$Q^2 = m_b^2$
$Q^2 = 4 m_b^2$
$\pi^- p \to b\bar{b} X$
$m_b = 5\,GeV$
200
400
600
800
Plab (GeV)

Fig. 3

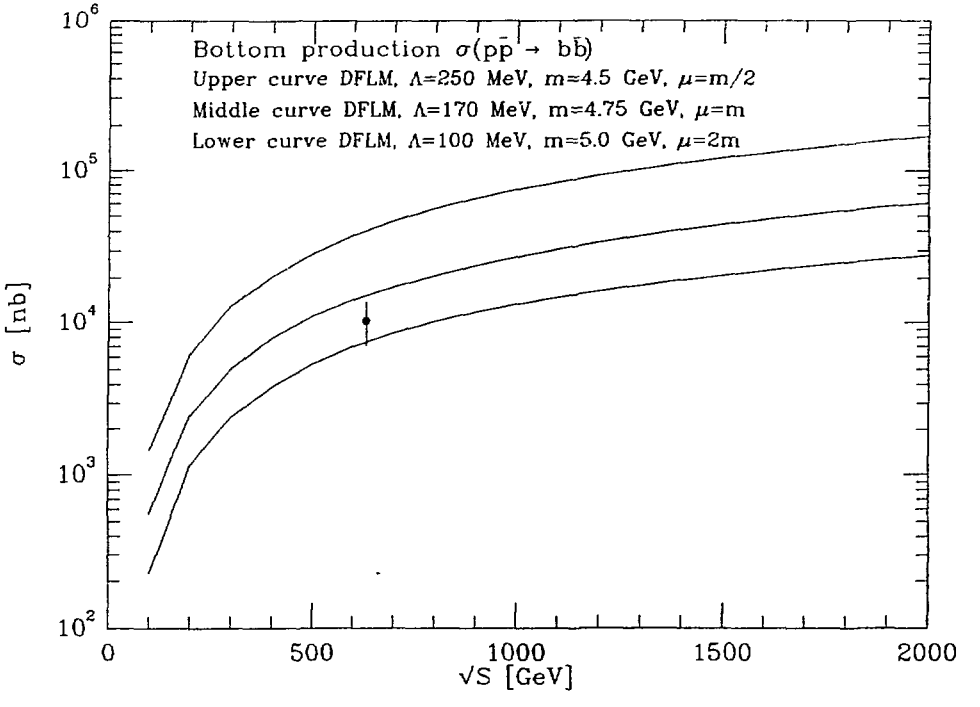
Bottom production σ(pp̄ → bb̄)
Upper curve DFLM, Λ=250 MeV, m=4.5 GeV, μ=m/2
Middle curve DFLM, Λ=170 MeV, m=4.75 GeV, μ=m
Lower curve DFLM, Λ=100 MeV, m=5.0 GeV, μ=2m
σ [nb]
10^6
10^5
10^4
10^3
10^2
0
500
1000
1500
2000
√S [GeV]

Fig. 4

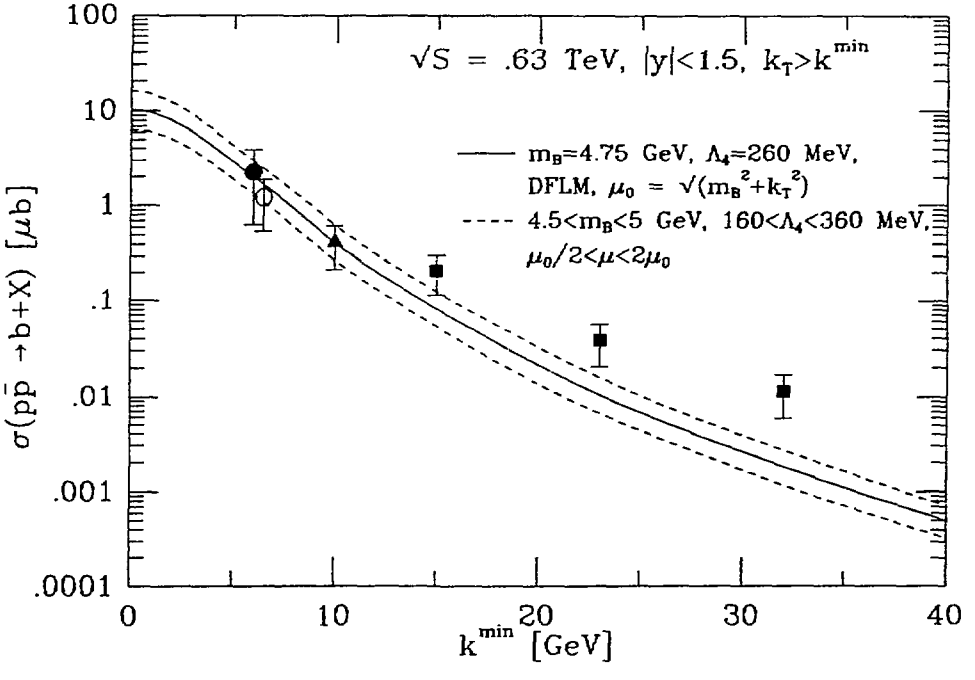
√S = .63 TeV, |y|<1.5, k_T>k^{min}
m_B=4.75 GeV, Λ_4=260 MeV,
DFLM, μ_0 = √(m_B^2+k_T^2)
4.5<m_B<5 GeV, 160<Λ_4<360 MeV,
$\mu_0/2<\mu<2\mu_0$
$\sigma(p\bar{p} \rightarrow b+X)$ [μb]
100
10
1
.1
.01
.001
.0001
0
10
20
30
40
k^{min} [GeV]

Fig. 5

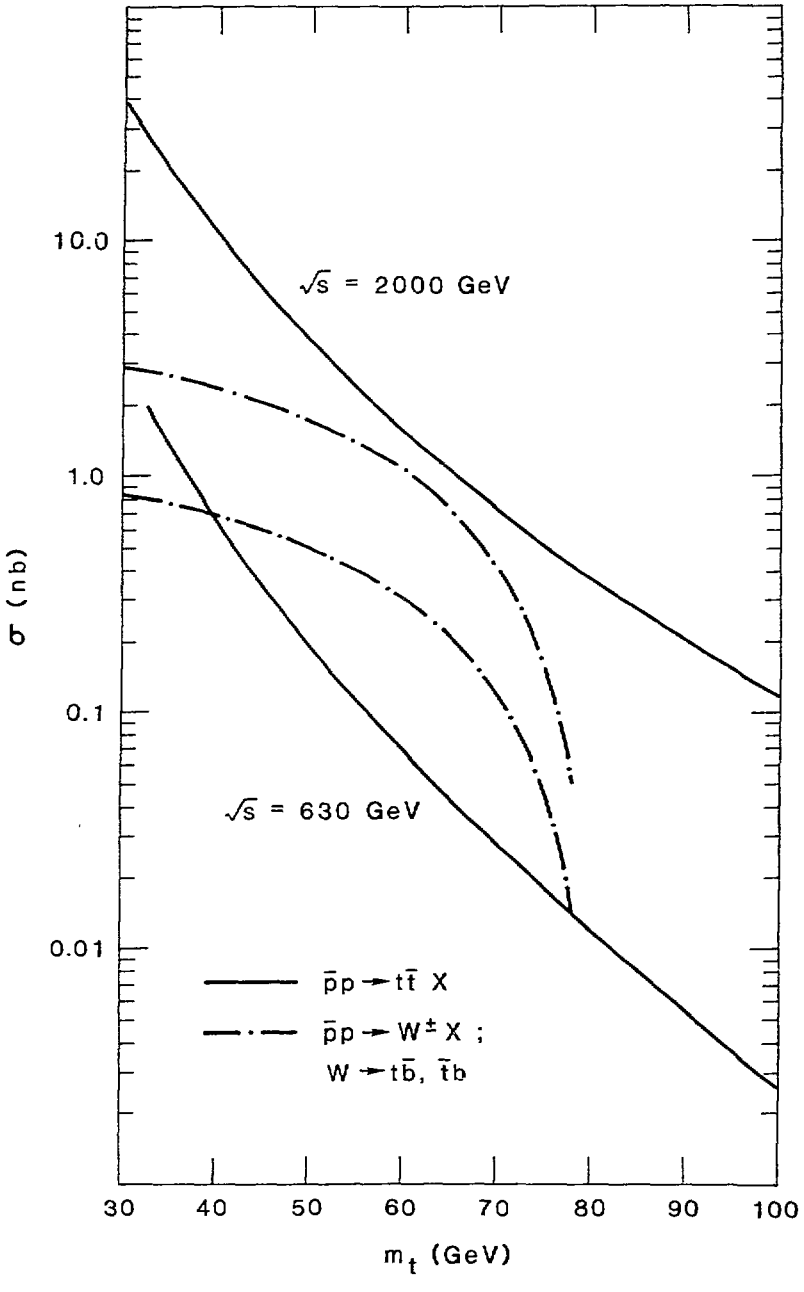
10.0
1.0
0.1
0.01
σ (nb)
√s = 2000 GeV
√s = 630 GeV
p̄p → tt̄ X
p̄p → W± X ;
W → tb̄, t̄b
30
40
50
60
70
80
90
100
m_t (GeV)

Fig. 6